Optical pulse propagation in doped fiber amplifiers

Govind P. Agrawal

The Institute of Optics, University of Rochester, Rochester, New York 14627

This paper provides a general treatment of the pulse-propagation problem in doped fiber amplifiers within the rate-equation approximation. The dopants are modeled as a two-level system whose dynamic response is governed by the population relaxation time T_1 and the dipole relaxation time T_2. For incident optical pulses with a width T_0 such that $T_1 \gg T_0 \gg T_2$, pulse amplification is governed by a Ginzburg-Landau-type equation that includes gain saturation, gain dispersion, fiber dispersion, fiber nonlinearity, and the detuning effects occurring when the carrier frequency of the input pulse does not coincide with the gain peak. In the absence of gain saturation, this equation has solitary-wave solutions in the form of chirped solitons. Our numerical results show that the chirped solitons are stable only in the normal-dispersion regime. In the case of anomalous dispersion, as is the case for erbium-doped fiber amplifiers, the amplified pulse develops many subpulses. The effect of gain saturation on pulse amplification is also discussed.

II. INTRODUCTION

The technique of doping silica fibers with rare-earth elements such as erbium, neodymium, and samarium provides an excellent gain medium that can be pumped optically to make lasers and amplifiers [1–19]. Although such lasers and amplifiers were studied [1,2] as early as 1961, they have attracted considerable attention only recently [4–19]. The current interest in erbium-doped fiber amplifiers is motivated mainly by their potential applications in fiber-optic communication systems [8–11]. From a fundamental standpoint, doped optical fibers offer practical realization of a two-level system in a dispersive nonlinear host [15–19] whose waveguiding property allows one to ignore the diffractive transverse effects which often complicate the study of other two-level systems. Many physical phenomena observed in quantum optics (self-induced transparency, photon echo, etc.) should be studied in doped optical fibers whose dispersive and nonlinear properties may lead to new qualitative features [13–19].

The objective of this paper is to provide a theoretical framework for the study of pulse propagation in doped fiber amplifiers. A basic propagation equation is derived in Sec. II by modeling the dopant response in terms of the population relaxation time T_1 and the dipole (or polarization) relaxation time T_2 of a two-level system. This equation is valid for incident optical pulses of width T_0 such that $T_1 \gg T_0 \gg T_2$, as is the case in most practical situations. The propagation equation includes the effects of gain saturation, gain dispersion, fiber dispersion, fiber nonlinearity, and atomic detuning. Sections III and IV solve this equation numerically without and with gain saturation, respectively, by considering the cases of anomalous and normal fiber dispersion. Particular attention is paid to the formation of chirped solitons. The main results are summarized in the concluding Sec. V.

II. BASIC PULSE-PROPAGATION EQUATION

The propagation of optical pulses in undoped single-mode fibers has been studied extensively, particularly in relation to optical solitons [20]. This study can be extended to include the effect of dopants. The analysis is simplified considerably if dopants are modeled as an ideal two-level atomic system. Mathematically, the response of a two-level atomic system is governed by the Bloch equations [21] and the associated population and dipole (polarization) relaxation times T_1 and T_2. The atomic system can be assumed to respond instantaneously if T_2 is much shorter than the pulse width T_0. For most dopants T_2 is in the range 50–100 fs whereas T_1 is ~ 1–10 ms. Since $T_2 \ll T_0$ for pulses as short as 1 ps, the atomic response for such pulses can be included through the susceptibility of a two-level system given by [21]

$$\chi_a(\omega) = \frac{g_p c}{\omega} \frac{(\omega - \omega_a)T_2 - i}{1 + (\omega - \omega_a)^2 T_2^2} , \tag{1}$$

where ω is the optical frequency, ω_a is the atomic resonance frequency, and the peak gain $g_p = \sigma(N_2 - N_1)$, where σ is the transition cross section and N_1 and N_2 are the atomic densities for the lower and upper energy levels of the two-level system. The rate equations for N_1 and N_2 can be used to obtain the following rate equation for the gain [21]:

$$\frac{dg_p}{dt} = \frac{g_0 - g_p}{T_1} - \left[\frac{2\sigma}{\hbar\omega} \right] g_p I , \tag{2}$$

where g_0 is the small-signal gain created by optical pumping and I is the optical intensity. The factor of 2 in Eq. (2) appears for two-level atoms whose lower level cor-

responds to the ground state [21]. This is the case for many dopants such as erbium. In the steady state Eq. (2) is readily solved to obtain $g_p = g_0/(I + I/I_s)$, where $I_s = \hbar\omega/(2\sigma T_1)$ is the saturation intensity. However, the steady-state solution can only be used either in the continuous-wave (cw) case or for long pulses such that $T_0 \gg T_1$. In most cases of practical interest $T_0 \ll T_1$, and the transient nature of gain must be included.

Equation (1) assumes that the gain profile is homogeneously broadened. In general, the response of dopants in optical fibers has an inhomogenous-broadening component because of the amorphous nature of silica glass [7]. For alumino-silicate glasses the inhomogenous contribution is small and T_2 in Eq. (1) can be related to the homogeneous line width $\Delta\omega_a = 2/T_2$. The inhomogenous component appears to be larger for germano-silicate glasses. For simplicity, we use Eq. (1) for all glasses with T_2 as a fitting parameter that is determined from the gain bandwidth.

The pulse-propagation problem in doped fibers can be solved by defining a complex dielectric constant as

$$\epsilon(\omega) = n_f^2(\omega) + 2in_f(c/\omega)\alpha_f + \chi_a(\omega) , \tag{3}$$

where α_f accounts for the fiber loss and n_f is the refractive index of the fiber. The fiber index n_f should include both linear and nonlinear contributions so that

$$n_f(\omega) = n(\omega) + n_2 I, \tag{4}$$

where the linear index n is different for the core and the cladding regions of the optical fiber. The frequency dependence of n_f and χ_a governs the dispersive effects associated with the fiber and the dopants, respectively. Furthermore, both n_f and χ_a are intensity dependent; the nonlinear effects result from such an intensity dependence. The application of Maxwell's equations leads to the following wave equation:

$$\nabla^2 \mathbf{E} - \mu_0 \frac{\partial^2 \mathbf{D}}{\partial t^2} = 0, \tag{5}$$

where $\mathbf{E}$ is the electric field vector, μ_0 is the vacuum permeability, and $\mathbf{D}$ is the displacement vector. The Fourier transform of $\mathbf{D}$ is related to that of $\mathbf{E}$ by the constitutive relation

$$\tilde{\mathbf{D}}(\mathbf{r},\omega) = \epsilon_0 \epsilon(\omega) \tilde{\mathbf{E}}(\mathbf{r},\omega), \tag{6}$$

where ϵ_0 is the vacuum permittivity and a tilde denotes the Fourier transform defined as

$$\tilde{\mathbf{E}}(\mathbf{r},\omega) = \int_{-\infty}^{\infty} \mathbf{E}(\mathbf{r},t) \exp(i\omega t) dt. \tag{7}$$

Equations (3)–(7) govern the propagation of electromagnetic field in any dispersive nonlinear medium. They are considerably simplified in the case of optical fibers because of the guided nature of the optical field. The electric field vector is written as

$$\mathbf{E}(\mathbf{r},t) = \tfrac{1}{2}\{\hat{e}F(x,y)A(z,t)$$

$$\times \exp[i(\beta_0 z - \omega_0 t)] + \text{c.c.}\}, \tag{8}$$

where $\hat{e}$ is the polarization unit vector, $F(x,y)$ is the field

distribution associated with the fundamental fiber mode, (HE_{11} mode), $A(z,t)$ is the complex amplitude of the pulse envelope, β_0 is the propagation constant at the carrier frequency ω_0, and c.c. stands for the complex conjugate. The optical field is assumed to remain linearly polarized along the same direction $\hat{e}$ during its propagation inside the fiber. This would be the case for polarization-preserving fibers with input polarization along one of its principle axes. The analysis, however, applies approximately even for conventional fibers.

Equations (3)–(8) can be used to obtain a basic propagation equation for the pulse envelope $A(z,t)$ by following the well-known techniques [20]. The dispersive effects are included by defining the propagation constant at the frequency ω as

$$\beta(\omega) = \sqrt{\epsilon(\omega)}\,\omega/c \tag{9}$$

and expanding it in a Taylor series in the vicinity of the carrier frequency ω_0. By substituting Eq. (3) in Eq. (9) and noting that α_f, $n_2 I$, and $|\chi_a|$ are much smaller than n, $\beta(\omega)$ is written as

$$\beta(\omega) = \beta_f(\omega) + \frac{\omega}{c} n_2 I + \frac{i}{2}\alpha_f + \frac{1}{2n}\chi_a(\omega), \tag{10}$$

where $\beta_f(\omega) = n(\omega)\omega/c$ is the propagation constant of the undoped fiber. The refractive index $n(\omega)$ stands for the model index.

Care must be exercised while expanding $\beta(\omega)$ in a Taylor series. Both n_2 and α_f vary with frequency, but the variation is slow enough that they can be treated as constants over the pulse bandwidths (typically ≤ 10 THz). However, this is not the case for the atomic susceptibility $\chi_a(\omega)$ governing the response of dopants. Because of a finite gain bandwidth, all spectral components do not experience the same gain, a phenomenon referred to as gain dispersion. Furthermore, if the carrier frequency of the incident field does not coincide with the gain peak located at ω_a, gain is accompanied by index changes which provide an additional contribution to the host dispersion governed by $n(\omega)$. The Taylor expansion of $\chi_a(\omega)$ in Eq. (1) yields the following expression:

$$\chi_a(\omega) = \frac{g_p}{2n_0}\left[\frac{\delta - i}{1 + \delta^2} + \frac{1 - \delta^2 + 2i\delta}{(1 + \delta^2)^2}(\omega - \omega_0)T_2 \right.$$

$$\left. + \frac{\delta(\delta^2 - 3) + i(1 - 3\delta^2)}{(1 + \delta^2)^3}(\omega - \omega_0)^2 T_2^2 \right], \tag{11}$$

where $n_0 = n(\omega_0)$, and we have introduced a detuning parameter δ by defining

$$\delta = (\omega_0 - \omega_a)T_2. \tag{12}$$

The effects of fiber dispersion are included by expanding $\beta_f(\omega)$ in a Taylor series and neglecting the cubic and higher-order terms, i.e.,

$$\beta_f(\omega) = \beta_0 + \beta_1(\omega - \omega_0) + \tfrac{1}{2}\beta_2(\omega - \omega_0)^2, \tag{13}$$

where $\beta_m = (d^m\beta/d\omega^m)_{\omega=\omega_0}$ for $m = 0$, 1, and 2. The pa-

rameter β_1 is related to the group velocity as $v_g = 1/\beta_1$. The parameter β_2 is called the group-velocity-dispersion parameter [20] since β_2 is proportional to $dv_g/d\omega$.

The propagation equation is obtained by solving Eq. (5) in the frequency domain with the help of Eqs. (6)–(8). In a simple approach, the Fourier component $\widetilde{A}(z,\omega)$ of $A(z,t)$ is found to evolve as [20]

$$\frac{\partial \widetilde{A}}{\partial z} = i\,[\beta(\omega) - \beta_0]\widetilde{A}, \tag{14}$$

where $\beta(\omega)$ is given by Eq. (10). By using Eqs. (11) and (13) and taking the inverse Fourier transform, $A(z,t)$ satisfies the propagation equation

$$\frac{\partial A}{\partial z} + \beta_1^{\text{eff}}\frac{\partial A}{\partial t} + \frac{i}{2}\beta_2^{\text{eff}}\frac{\partial^2 A}{\partial t^2}$$

$$= -\frac{\alpha_f}{2}A + \frac{g_p}{2n_0}\left[\frac{\delta - i}{1 + \delta^2}\right]A + i\gamma|A|^2A, \tag{15}$$

where

$$\beta_1^{\text{eff}} = \beta_1 + \frac{g_p T_2}{2n_0}\frac{1 - \delta^2 + 2i\delta}{(1 + \delta^2)^2}, \tag{16}$$

$$\beta_2^{\text{eff}} = \beta_2 + \frac{g_p T_2^2}{2n_0}\frac{\delta(\delta^2 - 3) + i(1 - 3\delta^2)}{(1 + \delta^2)^3}, \tag{17}$$

$$\gamma = n_2\omega_0/(ca_{\text{eff}}). \tag{18}$$

The amplitude A is normalized such that $|A|^2$ represents power. The nonlinearity coefficient γ in Eq. (18) contains the effective core area defined as

$$a_{\text{eff}} = \frac{\left[\int\int_{-\infty}^{\infty}|F(x,y)|^2dx\,dy\right]^2}{\int\int_{-\infty}^{\infty}|F(x,y)|^4dx\,dy}, \tag{19}$$

where $F(x,y)$ is the dimensionless spatial profile of the fundamental fiber mode. Typically a_{eff} is larger than the core area because of spreading of the fiber mode into the cladding. For single-mode fibers a_{eff} varies in the range 10–60 μm^2 depending on the operating wavelength and the core diameter.

Equation (15) together with Eq. (2) describes pulse propagation in doped optical fibers. A further simplification can be made by noting that in most practical applications of fiber amplifiers the pulse width is much smaller than the population relaxation time $(T_0 \ll T_1)$ as T_1 is ~ 1–10 ms for commonly used dopants such as erbium. As a result, the term containing T_1 in Eq. (2) can be neglected. Equation (2) can then be solved analytically with the result

$$g_p(z,t) = g_0 \exp\left[-\frac{1}{E_s}\int_{-\infty}^{t}|A(z,t)|^2dt\right], \tag{20}$$

where the saturation energy E_s is defined as

$$E_s = \hbar\omega_0 a_{\text{eff}}/2\sigma. \tag{21}$$

In obtaining Eq. (20), the intensity I in Eq. (2) was related to the pulse amplitude $A(z,t)$ as $I = |A|^2/a_{\text{eff}}$. Equation (20) governs saturation of the amplifier gain.

Gain saturation is important and must be included if the energy E_p of the amplified pulse becomes comparable to the saturation energy E_s. A curious feature of gain saturation is that both β_1^{eff} *and* β_2^{eff} become intensity dependent as they depend on $g_p(z,t)$ through the last term in Eqs. (16) and (17). The intensity dependence of β_1^{eff} implies that different parts of the pulse move at slightly different speeds. Such an intensity dependence can lead to pulse shaping. In practice, gain saturation is almost negligible for most doped fiber amplifiers since the saturation energy is relatively large $(E_s \sim 1\ \mu$J).

III. PULSE AMPLIFICATION WITHOUT GAIN SATURATION

To gain a physical understanding of the amplification process in fiber amplifiers, let us first consider the case of weak optical pulses whose energy remains well below the saturation level. The saturation energy of most dopants is quite large $(E_s \sim 1\ \mu$J). As an example $\sigma \sim 3 \times 10^{-21}$ cm^2 for erbium dopants [7]. By using $\hbar\omega_0 \sim 0.81$ eV at 1.53 μm and $a_{\text{eff}} = 50\ \mu$m^2, $E_s = 10.8\ \mu$J. Typical pulse energies for optical pulses used in fiber-optic communication systems are ~ 1 pJ. Even if such pulses are amplified by a factor of 1000 (30 dB), the output pulse energy remains well below E_s and gain saturation can be neglected. The exponential factor in Eq. (20) can then be approximated by 1, and g_p in Eqs. (15)–(17) can be replaced by its small-signal value g_0. For simplicity, let us also assume that the carrier frequency ω_0 of the incident pulse is matched exactly to the gain peak occurring at the atomic transition frequency ω_a so that $\delta = 0$ from Eq. (12). The parameter β_1^{eff} is then real and can be related to the effective group of the pulse as $v_g^{\text{eff}} = 1/\beta_1^{\text{eff}}$. By defining a reduced time as

$$T = t - \beta_1^{\text{eff}}z, \tag{22}$$

Eq. (15) can be written as

$$\frac{\partial A}{\partial z} + \frac{i}{2}\left[\beta_2 + \frac{ig_0T_2^2}{n_0}\right]\frac{\partial^2 A}{\partial T^2}$$

$$= \frac{1}{2}\left[\frac{g_0}{n_0} - \alpha_f\right]A + i\gamma|A|^2A, \tag{23}$$

where Eq. (17) was used. This equation reduces to the well-known nonlinear Schrödinger equation in the absence of fiber loss $(\alpha_f = 0)$ and the gain provided by dopants $(g_0 = 0)$. The nonlinear Schrödinger equation permits specific solutions, know as solitons [20], which correspond to optical pulses which either preserve their shape (the fundamental soliton) or follow a periodic evolution pattern (higher-order solitons) as they propagate inside the undoped fiber.

It is useful to normalize Eq. (23) by defining

$$U = A/(P_0)^{1/2}, \quad \tau = T/T_0, \quad \text{and} \quad \xi = z/L_D, \tag{24}$$

where P_0 is the peak power and T_0 is the width of the input pulse. The dispersion length L_D is defined as [20]

$$L_D = T_0^2 / |\beta_2| \ . \tag{25}$$

Solitons exist only in the anomalous dispersion region of the optical fiber where β_2 is negative. This is the case when the carrier wavelength $\lambda_0 = 2\pi c / \omega_0$ exceeds the so-called zero-dispersion wavelength λ_{ZD} of the fiber. For conventional fibers $\lambda_{ZD} \cong 1.3$ μm; it can be moved to the wavelength region near 1.55 μm in the especially designed dispersion-shifted fibers. Assuming $\beta_2 < 0$, Eq. (23) can be written in the normalized form

$$i\frac{\partial U}{\partial \xi} + \tfrac{1}{2}(1 - id)\frac{\partial^2 U}{\partial T^2} + N^2 |U| U = \frac{i}{2}\mu U, \tag{26}$$

where

$$d = \frac{g_0 T_2^2}{n_0 |\beta_2|}, \quad \mu = \left[\frac{g_0}{n_0} - \alpha_f\right] L_D. \tag{27}$$

The parameter N defined as

$$N = (\gamma P_0 L_D)^{1/2} = (\gamma P_0 T_0^2 / |\beta_2|)^{1/2} \tag{28}$$

is referred to as the soliton order. For undoped fibers the input pulse travels as a fundamental soliton when $N = 1$. From Eq. (28) the peak power and the width of fundamental solitons are related by

$$P_0 = |\beta_2| / \gamma T_0^2. \tag{29}$$

Typically $P_0 \approx 1-5$ W for $T_0 = 1$ ps. It is easy to verify that [20]

$$U(\xi, \tau) = \text{sech}(\tau) \exp(i\xi/2) \tag{30}$$

is a solution of Eq. (26) when $N = 1$ and the parameters d and μ are set to zero. Equation (30) shows that a pulse with the intensity profile $\text{sech}^2\tau$ would propagate without change in its shape as it propagates down the fiber. Such a shape-preserving soliton exists only for undoped fibers without any loss or gain so that the pulse energy is conserved along the fiber length.

For doped fiber amplifiers, pulse propagation is governed by Eq. (26). This equation differs from the nonlinear Schrödinger equation in two aspects. First, the pulse is amplified because of gain provided by dopants ($\mu > 0$). Second, the coefficient of the $\partial^2 U / \partial \tau^2$ term is complex because of gain dispersion. Equation (26) can be classified as a Ginzburg-Landau equation whose solutions have been extensively studied in many different contexts [22–24]. An interesting aspect of the Ginzburg-Landau equation is that it permits solitary-wave solutions in spite of the presence of the loss or gain that makes the underlying physical system non-conservative [23]. Indeed, a solitonlike solution of Eq. (26) is given by [25,26]

$$U(\xi, \tau) = \text{sech}(p\tau) \exp[iq \ln \cosh(p\tau) + i\Gamma\xi], \tag{31}$$

where p, q, and Γ are constants. These constants can be determined by substituting Eq. (31) in Eq. (26) and obviously depend on the gain-dispersion parameter d. A novel feature of the solution (31) is the presence of a time-dependent phase. Such pulses are called chirped, and the solitary-wave solution is referred to as a chirped soliton [15]. Another noteworthy feature of the solution (31) is

that both the soliton width and its peak power are uniquely determined by the gain-dispersion parameter d, or equivalently by T_2. This is in contrast with the solution (30) of the nonlinear Schrödinger equation for which P_0 and T_0 can vary as long as they are related such that $N = 1$ in Eq. (28). The gain term in Eq. (26) stabilizes only one soliton among the whole family and selects its size by breaking the scale invariance associated with the conservative problem [23].

The solitary-wave solution (31) is an eigensolution of the nonlinear propagation Eq. (26). In a practical situation, fiber amplifiers are used to amplify an input pulse of given width and peak power. Equation (26) can be used to describe the amplified pulse at the fiber output. We use the split-step Fourier method [20] to solve the initial-value problem numerically. The parameters μ and d are fixed by considering a fiber amplifier with the 10-dB gain per dispersion length L_D ($e^\mu = 10$ or $\mu \approx 2.3$) and by choosing an input pulse width T_0 such that $T_2/T_0 = 0.2$ ($d \approx 0.092$). The parameter N is related to the input peak power P_0 according to Eq. (20) and is varied over a wide range to understand the amplification process.

Consider first the amplification of a fundamental soliton by choosing $N = 1$ and solving Eq. (26) with the initial condition $U(0, \tau) = \text{sech}\tau$. Figure 1 shows pulse evolution over a distance $\xi = z/L_D = 2.5$ by displaying pulse shapes after every $L_D/2$. The most noteworthy feature of Fig. 1 is the dramatic pulse compression accompanying its amplification [27]. The compression stage is similar to that occurring for higher-order solitons [20]. It can be understood by noting that the initial stage of amplification of fundamental solitons raises the peak power such that N exceeds 1, and the pulse behaves as a higher-order soliton during the early stages of amplification. The extreme narrowing of the central peak can also be understood by noting that the pulse attempts to maintain N near 1 as it amplifies in order to propagate as a fundamental soliton. From Eq. (28) the pulse width
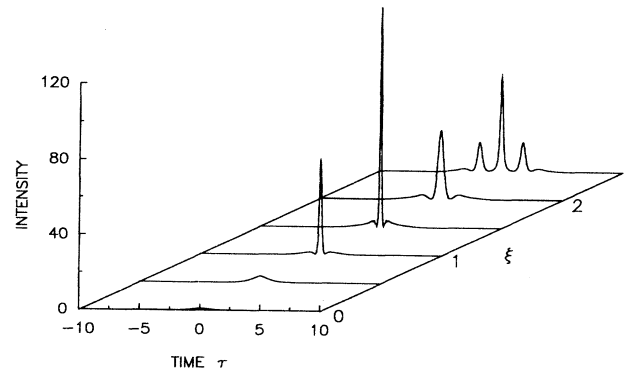

FIG. 1. Evolution of fundamental soliton ($N = 1$) in a doped fiber with 10-dB gain per dispersion length ($\mu = 2.3$). At fiber input $U(0, \tau) = \text{sech}\tau$, where $\tau = T/T_0$ is the normalized time and pulse width T_0 is chosen such that $T_2/T_0 = 0.2$ ($d = 0.092$). The propagation distance $\xi = z/L_D$ where L_D is the dispersion length.
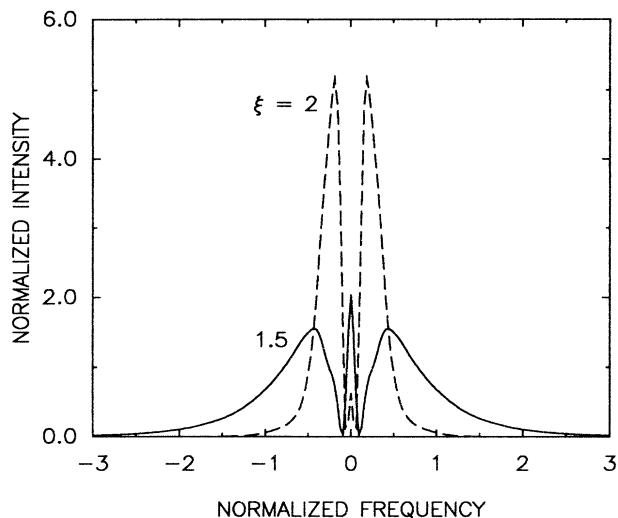
FIG. 2. Pulse spectra at $\xi = 1.5$ and 2 for parameter values of Fig. 1. Spectral narrowing at $\xi = 2$ is due to gain dispersion; it is responsible for pulse broadening seen in Fig. 1 when the pulse propagates from $\xi = 1.5$ to 2.

T_0 decreases as $P^{-1/2}$ where P is the peak power.

The compression stage cannot continue indefinitely because of the presence of gain dispersion. When the pulse becomes so short that its spectrum exceeds the gain bandwidth, spectral wings are amplified less than the central peak. As a result, pulse spectrum narrows, and pulse width increases. Gain-dispersion-induced broadening is evident in Fig. 1 if we compare the pulse shapes at $\xi = 1.5$ and 2. The corresponding spectra are shown in Fig. 2 where spectral narrowing occurring when the pulse propagates from $\xi = 1.5$ to 2 is clearly seen. The optical pulse is also considerably chirped because of gain dispersion. Figure 3 shows the frequency chirp defined as
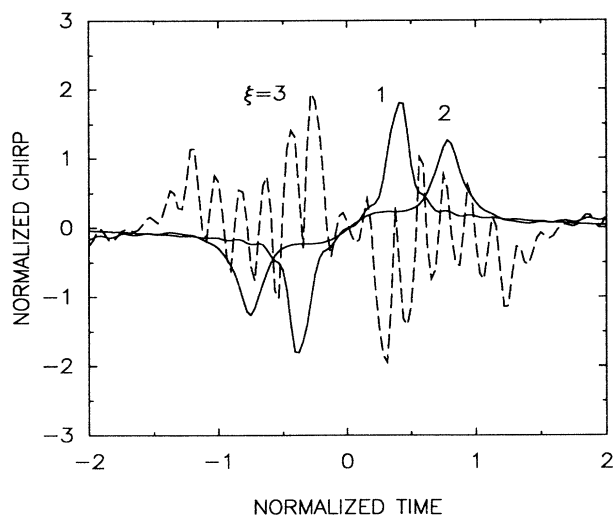

FIG. 3. Frequency chirp $\Delta \nu$ across the pulse at $\xi = 1$, 2, and 3. The chirp is absent at the amplifier input ($\Delta \nu = 0$) Parameter values are the same as for Fig. 1.

$$\Delta \nu = -\frac{1}{2\pi} \frac{\partial \phi}{\partial \tau}, \tag{32}$$

where ϕ is the phase of $U(\xi, \tau)$. The chirp profile changes considerably along the fiber length. In particular, the chirp behavior is qualitatively different beyond $\xi = 2$ as is evident by rapid oscillations seen in Fig. 3 for $\xi = 3$.

The qualitative changes beyond $\xi = 2$ can be attributed to the generation of additional subpulses in the time domain. Figure 1 shows the appearance of such subpulses at $\xi = 2.5$. The number and the amplitude of subpulses grow with further propagation. Figure 4 shows the pulse shapes and spectra at $\xi = 3$ and 5. The number of subpulses has grown to 7 at $\xi = 5$ and keeps increasing with further propagation. Each subpulse has about the same width and about the same amplitude. The spacing between the subpulses is nearly uniform (except for the subpulses near the boundary that are still in the process of formation) and does not change with propagation.

How can one understand such a behavior? A partial answer lies in the solitary-wave solution. Eq. (31), associated with the Ginzburg-Landau equation (26). The width and the peak power of each subpulse are determined by the gain-dispersion parameter d or T_2/T_0. The input pulse evolves toward the chirped soliton. However, once it attains the required peak power, it cannot amplify any further. This appears to be the case near $\xi = 2$ in Fig. 1. Beyond $\xi = 2$, the fiber amplifier supplies energy to the pedestal that accompanies the pulse. Each subpulse grows out of such pedestal amplification. From a physical standpoint a steady state is not reached simply because the amplifier continues to provide gain, and small fluctuations are amplified and shaped to become chirped solitons. Figure 5 shows how the energy E_p and the root-mean-square width (rms) σ_p (of the entire pulse train) increase with distance. They are defined as

$$E_p(\xi) = \int_{-\infty}^{\infty} |U(\xi, \tau)|^2 d\tau,$$

$$\sigma_p^2(\xi) = \int_{-\infty}^{\infty} \tau^2 |U(\xi, \tau)|^2 d\tau, \tag{33}$$

and are normalized to 1 at the input ($\xi = 0$). The pulse energy E_p increases tenfold (by 10 dB) within one dispersion length, oscillates from $\xi = 1$ and 2 as the compressed pulse tries to form a chirped soliton, and then increases once again beyond $\xi = 2$ as the new subpulses are formed. From a fundamental standpoint, the chirped soliton given by Eq. (31) is not stable against perturbations.

One may wonder what happens if the optical pulse propagates in the normal-dispersion regime of fiber amplifiers. The solitary-wave solutions of the Ginzburg-Landau equation exist in the form of a chirped soliton even in the case of normal dispersion ($\beta_2 > 0$). Our numerical simulations show that the input pulse amplifies and evolves toward this chirped soliton just as it does in the case of anomalous dispersion. Interestingly enough, it stabilizes when β_2 is positive, and no subpulses are generated. Figure 6 shows the variation of pulse energy E_p and the rms width σ_p along the fiber length and should

be compared with Fig. 5. Both E_p and σ_p have become constant for $\xi \gg 1$ indicating that the pulse has evolved toward a stable chirped soliton. The origin of soliton stability in the normal-dispersion case is not clear and requires further investigation. A partial explanation is that the input pulse broadens in the case of normal dispersion rather than undergoing compression as is the case for anomalous dispersion. As a result, it encompasses any radiation generated during the evolution phase. By contrast, the radiation generated in the case of anomalous dispersion is separated from the main pulse and seeds the instability.

Before leaving this section, let us consider briefly the case in which the carrier frequency ω_0 and the gain-peak frequency ω_a do not coincide so that the parameter δ given by Eq. (12) is nonzero. Such detuning effects can be studied by solving Eq. (15). The main difference is that the amplifier gain is accompanied by an index change whose magnitude depends on δ. Both β_1^{eff} and β_2^{eff} become δ dependent. A new qualitative feature is that β_1^{eff} becomes complex. The imaginary part of β_1^{eff} leads to a

shift of the pulse spectrum toward the gain peak. This behavior can be understood qualitatively by noting that when the peaks of the pulse and gain spectra do not coincide, the spectral peak of the pulse at ω_0 experiences less gain than the spectral components located near ω_a. This feature leads to a pulling of the pulse spectrum toward the gain peak.

IV. PULSE AMPLIFICATION WITH GAIN SATURATION

This section considers the effect of gain saturation on soliton amplification in fiber amplifiers. Pulse evolution is governed by Eq. (15), but the gain g_p is now time dependent and is given by Eq. (20). By using the normalized parameters given by Eqs. (22) and (24), Eq. (15) can be written as

$$i\frac{\partial U}{\partial \xi} + \frac{1}{2}(1 - id')\frac{\partial^2 U}{\partial \tau^2} + N^2|U|^2 U = \frac{i}{2}\mu' U \qquad (34)$$
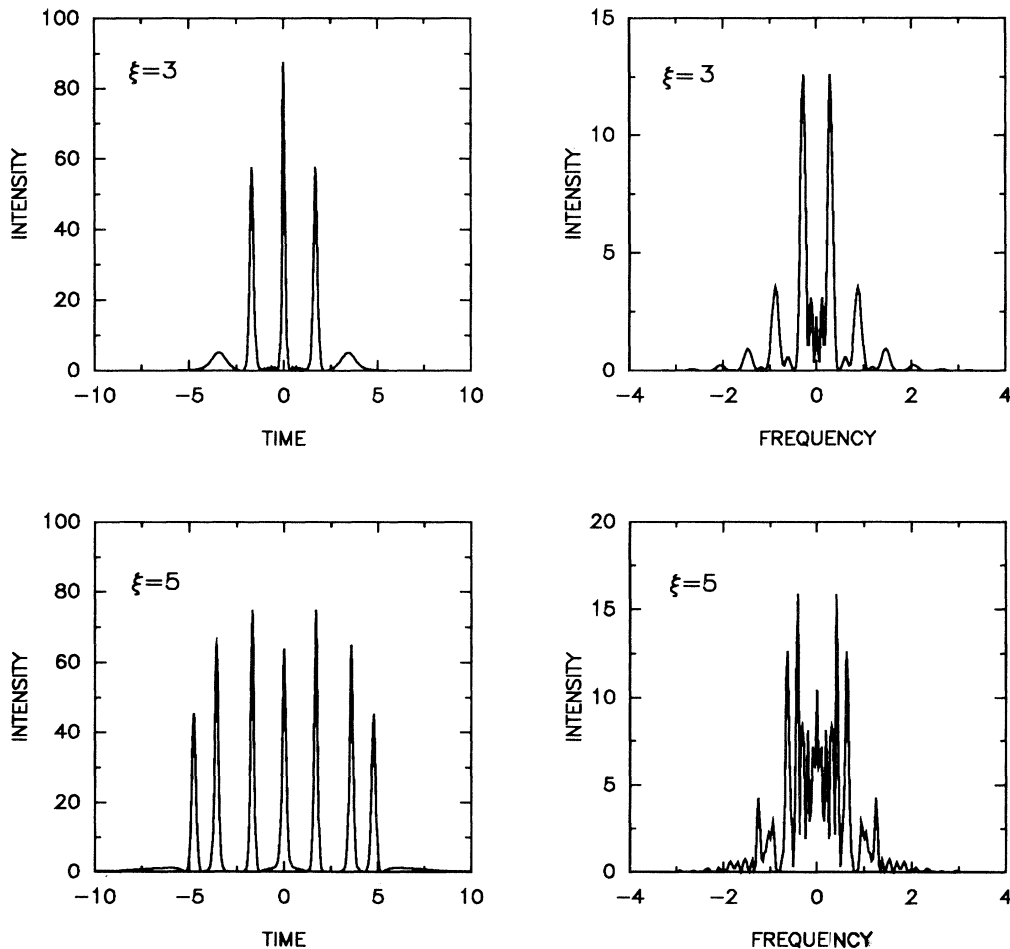
where

FIG. 4. Pulse shapes and pulse spectra at $\xi = 3$ and 5 for the case shown in Fig. 1. New subpulses are generated continuously as the pulse propagates along the fiber amplifier.
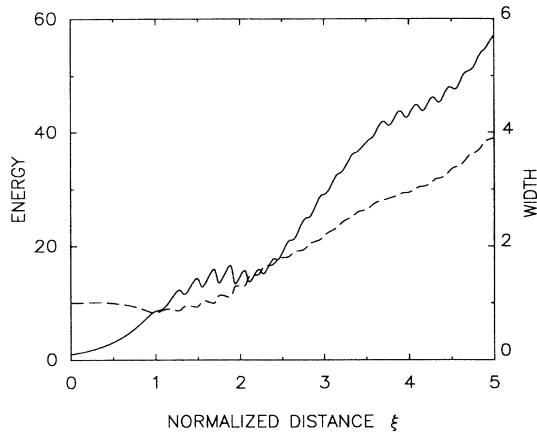
FIG. 5. Energy (solid line) and rms width (dashed line) of the amplified pulse (including subpulses) as a function of the propagation distance. Parameter values are the same as for Fig. 1.

$$d' = d \exp\left[-s \int_{-\infty}^{\tau} |U|^2 d\tau \right],$$

$$\mu' = \mu \exp\left[-s \int_{-\infty}^{\tau} |U|^2 d\tau \right], \tag{35}$$

d and μ are defined as in Eq. (27), and the new saturation parameter s is given by

$$s = P_0 \tau_0 / E_s. \tag{36}$$

In the absence of gain saturation ($s \ll 1$), $d' \approx d$, $\mu' \approx \mu$, and Eq. (34) reduces to Eq. (26), as it should. The effect of gain saturation is to make the parameters d' and μ' time dependent through their dependence on the intensity. For most fiber amplifiers $s \ll 1$ under typical operating conditions as the saturation energy is relatively large compared with the input pulse energy. To illustrate the gain-saturation effects we choose $s = 0.01$.

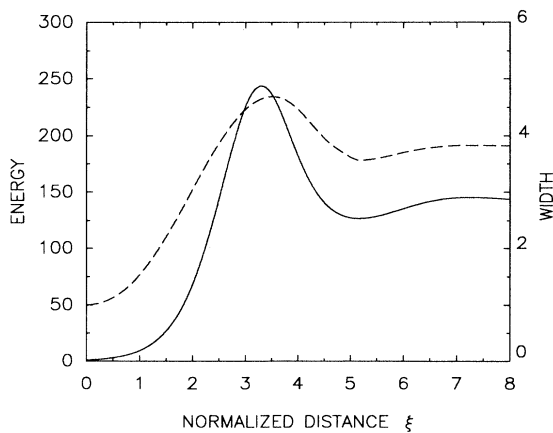Figure 7 shows the temporal profiles of the amplified

FIG. 6. Energy (solid line) and rms width (dashed line) when the input pulse propagates in the normal-dispersion region of the fiber amplifier. All other parameter values are the same as in Fig. 1.
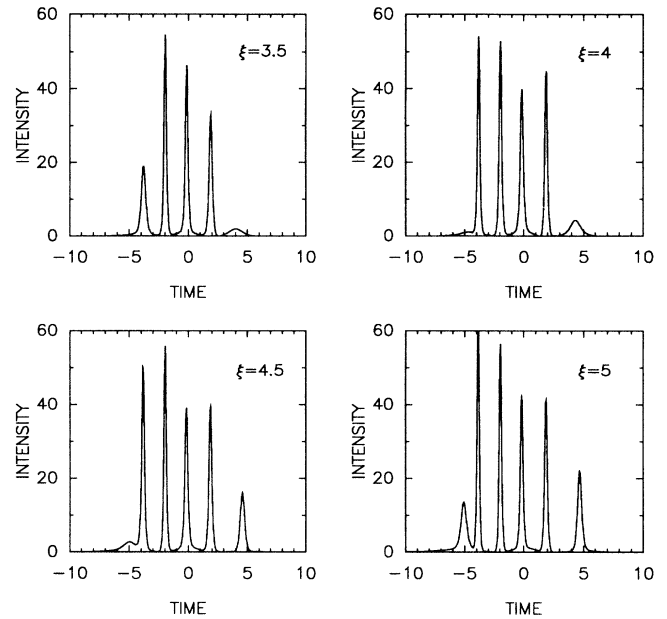

FIG. 7. Pulse shapes for ξ in the range 3.5–5 for the case of anomalous dispersion. Parameter values are the same as in Fig. 1 except that gain saturation is included by choosing $s = 0.01$.

pulse by using parameter values identical to those used for Figs. 1–4 except that the gain-saturation effects are included by using $s = 0.01$. Specifically, the input pulse corresponds to a fundamental soliton ($N = 1$) and propagates in the anomalous-dispersion regime of the fiber amplifier. The amplification process is qualitatively similar to the case $s = 0$ (no gain saturation) in the sense that the input pulse splits into many pulses. The new qualitative feature is that the temporal profile of the amplified pulse becomes asymmetric. This asymmetry has its origin in gain saturation and can be understood as follows. The leading edge of the pulse ($\tau < 0$) experiences more gain than the trailing edge since it experiences nearly unsaturated gain. The gain is reduced by the time the trailing edge arrives because of gain saturation induced by the leading edge. Each subpulse in Fig. 7 can still be interpreted as a chirped soliton whose width and peak power are determined by the saturated value of the local gain. It is noteworthy that the pulse amplification process is affected by values of the gain-saturation parameter as small as $s = 0.01$.

One would expect that the gain saturation would also affect pulse amplification in the normal-dispersion regime ($\beta_2 < 0$) of the fiber. In particular, the amplified pulse may not be able to form a stable chirped soliton as was the case in the absence of gain saturation. This indeed turns out to be the case. Figure 8 shows the pulse profiles in the range $\xi = 0$–8 by using the parameter values identical with those of Fig. 7 except that β_2 is now taken to be positive. A comparison of pulse shapes in Figs. 7 and 8 reveals the dramatic difference between the normal-dispersion ($\beta_2 > 0$) and anomalous-dispersion ($\beta_2 < 0$) regimes. The amplified pulse tries to form a chirped soli-
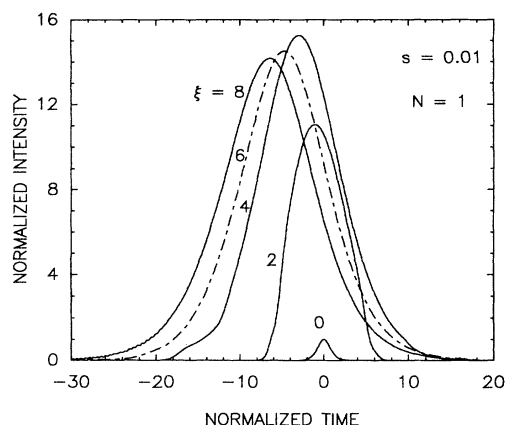
FIG. 8. Pulse shapes for ξ in the range 0–8 for the case of normal dispersion. All other parameter values are identical to those used for Fig. 7.

ton. However, stability of this soliton is lost because of the presence of gain saturation. Since the leading edge experiences more gain than the traveling edge, the peak of the amplified pulse moves continuously toward the leading edge. The pulse shape also becomes asymmetric with a relatively long leading edge.

V. CONCLUDING REMARKS

This paper has attempted to provide a general treatment of the pulse-propagation problem in doped fiber amplifiers within the rate-equation approximation. The dopants are modeled as a two-level system whose dynamic response is governed by the population relaxation time T_1 and dipole (or polarization) relaxation time T_2. For most dopants, T_1 is in the range 1–10 ms whereas T_2 is extremely short ($T_2 \sim 50$ fs). In most cases of practical interest, the input pulse width T_0 is expected to be such that $T_1 \gg T_0 \gg T_2$. The amplification of such pulses is governed by our main propagation equation [Eq. (15)] which includes gain saturation, gain dispersion, fiber dispersion, fiber nonlinearity, as well as the detuning effects occurring when the carrier frequency of the input pulse does not coincide with the gain peak. In the absence of gain saturation this equation reduces to a Ginzburg-Landau equation and has special solitary-wave solutions in the form of chirped solitons. We have used this equation to study numerically the amplification of fundamental solitons in the anomalous-dispersion regime of the fiber amplifier. An important result is that the amplified pulse does not form a stable chirped soliton as one might have expected. Instead, the amplified pulse takes the form of a pulse train whose individual subpulses can be interpreted approximately as chirped solitons. This qualitative behavior remains unchanged even in the presence of gain saturation. The amplification process is found to be drastically different if the input pulse propagates in the normal-dispersion regime of the fiber. In the absence of gain saturation, the amplified pulse evolves toward a chirped soliton that is a solution of the underlying Ginzburg-Landau equation. Surprisingly, the chirped soliton is stable in the case of normal dispersion in contrast with the anomalous-dispersion case where new subpulses are continuously generated. It would be of considerable interest to observe experimentally stable solitons in the normal-dispersion region of doped optical fiber. Optical fibers doped with Nd^{3+} are most promising for such an observation [28–30].

ACKNOWLEDGMENTS

[1] E. Snitzer, J. Appl. Phys. 32, 36 (1961); Phys. Rev. Lett. 7, 444 (1961).

[2] C. J. Koester and E. Snitzer, Appl. Opt. 3, 1182 (1964).

[3] J. Stone and C. A. Burrus, Appl. Phys. Lett. 23, 388 (1973).

[4] S. B. Poole, D. N. Payne, R. J. Mears, M. E. Ferrmann, and R. I. Lanning, J. Lightwave Technol. LT - 4, 870 (1986).

[5] R. J. Mears, L. Reekie, I. M. Jauncey, and D. N. Payne, Electron. Lett. 23, 1026 (1987).

[6] E. Desurvire, J. R. Simpson, and P. C. Becker, Opt. Lett. 12, 888 (1987).

[7] C. R. Giles and E. Desurvire, J. Lightwave Technol. 9, 147 (1991); 9, 271 (1991).

[8] S. Saito, T. Imai, and T. Ito, J. Lightwave Technol. 9, 161 (1991).

[9] G. R. Walker, N. G. Walker, R. C. Steele, M. J. Creaner, and M. C. Brain, J. Lightwave Technol. 9, 182 (1991).

[10] L. F. Mollenauer, S. G. Evangelides, and H. A. Haus, J. Lightwave Technol. 9, 194 (1991).

[11] K. Nakagawa, S. Nishi, K. Aida, and E. Yoneda, J. Lightwave Technol. 9, 198 (1991).

[12] B. J. Ainslie, J. Lightwave Technol. 9, 220 (1991).

[13] I. Yu. Khrushchev, A. B. Grudinin, E. M. Dianov, D. V. Korobkin, V. A. Semenov, and A. M. Prokhorov, Electron. Lett. 26, 456 (1990).

[14] M. Nakazawa, K. Kurokawa, H. Kubota, and E. Yamada, Phys. Rev. Lett. 65, 1881 (1990).

[15] G. P. Agrawal, IEEE Photon. Technol. Lett. 2, 875 (1990).

[16] V. Petrov and W. Rudolph, Opt. Commun. 76, 53 (1990).

[17] I. V. Melnikov, R. F. Nabiev, and A. V. Nazarkin, Opt. Lett. 15, 1348 (1990).

[18] G. P. Agrawal, Opt. Lett. 16, 226 (1991).

[19] M. Nakazawa, E. Yamada, H. Kubota, and H. A. Haus, Phys. Rev. A 44, 5973 (1991).

[20] G. P. Agrawal, Nonlinear Fiber Optics (Academic, Boston, 1989).

[21] A. E. Siegman, Lasers (University Science Books, Mill Valley, CA, 1986).

[22] For a review, see R. J. Deissler, J. Stat. Phys. 54, 1459 (1989), and references cited therein.

[23] S. Fauve and O. Thual, Phys. Rev. Lett. 64, 282 (1990).

[24] W. Van Saarloos and P. C. Hohenberg, Phys. Rev. Lett. 64, 749 (1990).

[25] C. S. Bretherton and E. A. Spiegel, Phys. Lett. 96A, 152 (1983).

[26] P. A. Bélanger, L. Gagnon, and C. Paré, Opt. Lett. **14**, 943 (1989).

[27] K. J. Blow, N. J. Doran, and D. Wood, J. Opt. Soc. Am. B **5**, 381 (1988).

[28] R. J. Mears, L. Reekie, S. B. Poole, and D. N. Payne, Electron. Lett. **21**, 738 (1985).

[29] I. M. Jauncey, L. Reekie, J. E. Townsend, D. N. Payne, and C. J. Rowe, Electron. Lett. **24**, 24 (1988).

[30] I. N. Duling, L. Goldberg, and J. F. Weller, Electron. Lett. **24**, 1333 (1988).